

Modeling the Photosynthetic Water Oxidation Complex: Activation of Water by Controlled Deprotonation and Incorporation into a Tetranuclear Manganese Complex

Guillem Aromí,[†] Michael W. Wemple,[†] Sheila J. Aubin,[‡]
Kirsten Foltling,[†] David N. Hendrickson,^{*,‡} and
George Christou^{*,†}

Department of Chemistry and Molecular Structure Center
Indiana University, Bloomington, Indiana 47405-4001
Department of Chemistry, 0358, University of California
at San Diego, La Jolla, California 92093-0358

Received September 2, 1997

Elucidating the structure and mechanism of action of the predominantly carboxylate-ligated, oxide-bridged Mn₄ cluster at the water oxidation center (WOC) of plants and cyanobacteria is of great current interest.^{1,2} This cluster binds, deprotonates, and oxidatively couples two H₂O molecules to yield O₂, but the precise details of this transformation are unclear. Recently, we have developed preparative methodology to the Mn^{III}Mn^{IV} complexes [Mn₄O₃X(O₂CMe)₃(dbm)₃] (X⁻ = Cl⁻, Br⁻, PhCO₂⁻, MeCO₂⁻; dbmH = dibenzoylmethane) containing the [Mn₄O₃] oxide-bridged trigonal pyramidal Mn₄ core that is one of the topologies consistent with recent EXAFS data on the native site,⁴ which has both short (~2.7 Å) and long (~3.3 Å) Mn...Mn separations. A major objective is to employ these model complexes to obtain structural and mechanistic insights into the interaction of the native cluster with its cofactors (Cl⁻, Br⁻, NO₃⁻, etc.), inhibitors (F⁻, NH₃, RNH₂, ROH), and substrate (H₂O);¹ we have shown, for example, that [Mn₄O₃(O₂CMe)₄(dbm)₃] (**1**) readily reacts with a F⁻ source to give [Mn₄O₃F(O₂CMe)₃(dbm)₃].^{3c} Understanding the means by which a Mn₄ cluster binds, deprotonates, and oxidizes H₂O molecules is the primary objective, and we are attempting to use model complexes to achieve this in a stepwise fashion that might allow intermediates to be identified and thus provide insights into how such a transformation might proceed. In the present work, we report that **1** will spontaneously react with H₂O under mild, nonforcing conditions leading to deprotonation of the latter and its incorporation into the core. This reaction represents a controlled activation of H₂O and is proposed as a model system for the crucial first steps along the path to O₂ evolution.

The reactivity of **1** with H₂O and MeOH was conveniently monitored by ²H NMR spectroscopy using [Mn₄O₃(O₂CCD₃)₄(dbm)₃] (**1a**); this avoids the complicating presence of dbm resonances and gives sharper resonances than ¹H NMR spectroscopy. In addition to the signal for CH₂Cl₂ impurity, the spectrum of **1a** at room temperature shows two signals at 36.8 and 66.1 ppm in a 3:1 integration ratio from the μ-O₂CCD₃ and unique μ₃-O₂CCD₃ groups, respectively (Figure 1, top). Addition of distilled MeOH causes a decrease in these two signals and

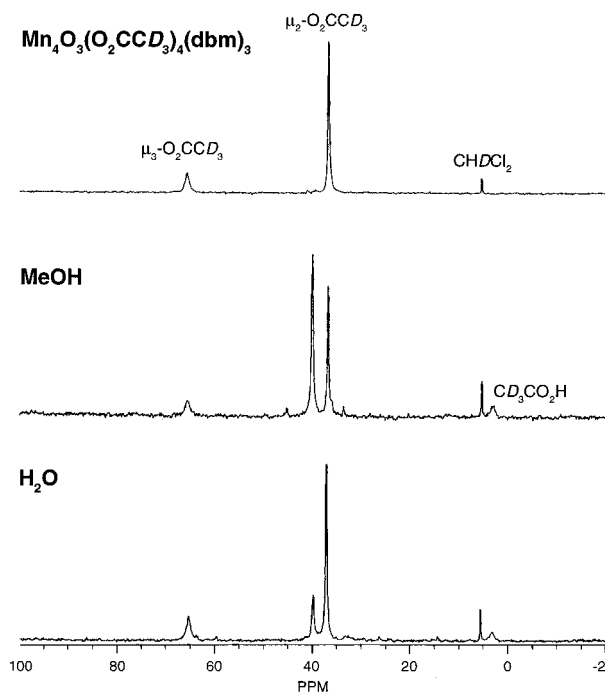
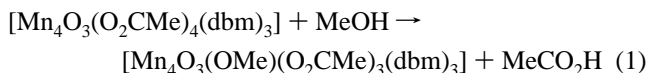


Figure 1. ²H NMR spectrum at ~23 °C of complex **1a** in CD₂Cl₂ (top); spectrum resulting from addition of 10 equiv of MeOH (middle); spectrum resulting from addition of an excess (immiscible) of H₂O (bottom).

appearance of free CD₃CO₂H at ~3 ppm and a new resonance at 39.7 ppm (Figure 1, middle). Addition of more MeOH causes an increase in the latter two signals at the expense of the former two. These data suggest a site-specific ligand substitution of the unique acetate group to give [Mn₄O₃(OMe)(O₂CCD₃)₃(dbm)₃] (**2a**). Similarly, addition of an excess of distilled H₂O (only sparingly miscible in CD₂Cl₂) causes analogous spectral changes with a new resonance appearing at 39.5 ppm (Figure 1, bottom), again suggesting displacement of the unique μ₃-CD₃CO₂⁻ group and possible formation of [Mn₄O₃(OH)(O₂CCD₃)₃(dbm)₃] (**3a**). Firm identification of these two products followed from their bulk isolation and structural characterization.

Complex **1** was dissolved in CH₂Cl₂ containing ~300 equiv of MeOH, the solvent removed in vacuo, the cycle repeated, and the residue again dissolved in CH₂Cl₂/MeOH; the product was precipitated with Et₂O, filtered, and dried in vacuo to give [Mn₄O₃(OMe)(O₂CMe)₃(dbm)₃] (**2**) in ~50% yield (eq 1). With



the identity of **2** established,^{5,6} its reaction with H₂O was found to provide a more convenient route to **3**. Thus, **2** was twice treated to cycles of dissolution in CH₂Cl₂/MeCN (7:1) containing 30 equiv of H₂O, followed by precipitation of the solid with Et₂O. The final solid of [Mn₄O₃(OH)(O₂CMe)₃(dbm)₃] (**3**) was obtained in 55–60% yield (eq 2).⁷

(5) Dried solid analyzed as 2·1/4CH₂Cl₂. Anal. Calcd (found): C, 53.8 (53.8); H, 4.1 (4.0). Crystal data for 2·2CH₂Cl₂: monoclinic, P2₁/c, a = 14.278(5) Å, b = 15.108(6) Å, c = 27.500(12) Å, β = 100.51(2)°, Z = 4, V = 5832 Å³, d_{calc} = 1.498 g cm⁻³, T = -171 °C; R(F) = 9.82 and R_w(F) = 8.77% using 5203 unique reflections with F > 3σ(F).

(6) Pure **2a** was made in a similar fashion from **1a**. The ²H NMR spectrum of **2a** exhibits only the 39.7 ppm resonance, confirming **2a** as the product of the methanolysis in Figure 1, middle.

(7) Pure **3a** was made in a similar fashion from **2a**. The ²H NMR spectrum of **3a** exhibits only the 39.5 ppm resonance, confirming **3a** as the product of the hydrolysis in Figure 1, bottom.

[†] Indiana University.

[‡] University of California at San Diego.

(1) (a) Debus, R. J. *Biochim. Biophys. Acta* **1992**, *1102*, 269. (b) *Manganese Redox Enzymes*; Pecoraro, V. L., Ed.; VCH Publishers: New York, 1992.

(2) (a) Ruettinger, W. F.; Dismukes, G. C. *Chem. Rev.* **1997**, *97*, 1. (b) Manchandra, R.; Brudvig, G. W.; Crabtree, R. *Coord. Chem. Rev.* **1995**, *144*, 1.

(3) (a) Wang, S.; Tsai, H.-L.; Foltling, K.; Streib, W. E.; Hendrickson, D. N.; Christou, G. *Inorg. Chem.* **1996**, *35*, 7578. (b) Wang, S.; Tsai, H.-L.; Hagen, K. S.; Hendrickson, D. N.; Christou, G. *J. Am. Chem. Soc.* **1994**, *116*, 8376. (c) Wemple, M. W.; Adams, D. M.; Foltling, K.; Hendrickson, D. N.; Christou, G. *J. Am. Chem. Soc.* **1995**, *117*, 7275.

(4) (a) DeRose, V. J.; Mukerji, I.; Latimer, M. J.; Yachandra, V. K.; Sauer, K.; Klein, M. P. *J. Am. Chem. Soc.* **1994**, *116*, 5239 and references therein. (b) Yachandra, V. K.; DeRose, V. J.; Latimer, M. J.; Mukerji, I.; Sauer, K.; Klein, M. P. *Science* **1993**, *260*, 675.

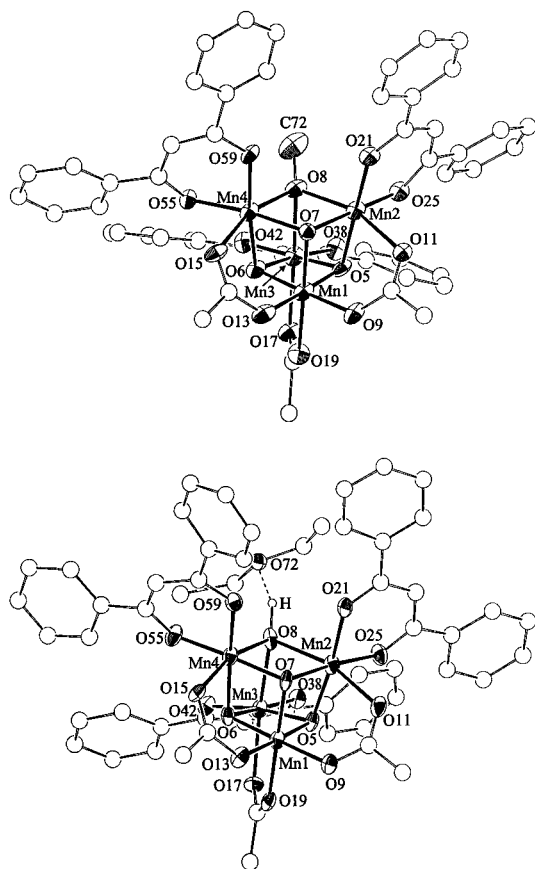
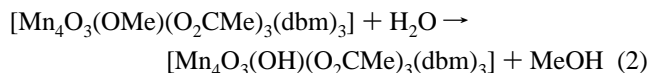


Figure 2. ORTEP representations of complexes **2** (top) and **3** (bottom) at the 50% probability level.

Table 1. Comparison of $[\text{Mn}_4\text{O}_3\text{X}]^{6+}$ Core Distances in Complexes **1–3**^{a–c}

	1	2	3
Mn ^{III} ...Mn ^{IV}	2.799(12)	2.798(6)	2.789(2)
Mn ^{III} ...Mn ^{III}	3.201(12)	3.132(26)	3.122(17)
Mn ^{III} –O _X	2.299(21)	2.182(23)	2.215(39)
Mn ^{III} –O _b	1.933(21)	1.936(23)	1.930(25)
Mn ^{IV} –O _b	1.867(9)	1.862(9)	1.862(12)

^a Averaged using C_{3v} virtual symmetry. ^b Numbers in parentheses are the greatest deviations of single values from the mean. ^c Mn(1) is Mn^{IV}; Mn(2), Mn(3), and Mn(4) are Mn^{III}; O_X = O of μ_3 -MeCO₂[–], MeO[–], or HO[–]; O_b = μ_3 -O^{2–} ions.



The structures of **2**⁵ and **3**⁸ (Figure 2) show great similarity to that of **1** except that the μ_3 -O₂CMe[–] is replaced by μ_3 -OMe[–] or OH[–] groups: in each case there is a Mn^{III}₃Mn^{IV} trigonal pyramid whose Mn^{III}₃ basal face is capped by a μ_3 -X[–] (X[–] = O₂CMe[–], OMe[–], OH[–]) group and its other faces by μ_3 -O^{2–} to give a highly distorted cubane $[\text{Mn}_4\text{O}_3\text{X}]^{6+}$ core. Interatomic distances (Table 1) confirm retention of both “short” (~2.8 Å) and “long” (3.1–3.2 Å) Mn...Mn separations in **2** and **3**; indeed, variation of X[–] causes almost insignificant changes to the structure of the core. Note that the $[\text{Mn}_4\text{O}_3(\text{OH})]^{6+}$ core of **3** is different from the more symmetric $[\text{Mn}_4\text{O}_4]^{6+}$ cubane core of $[\text{Mn}_4\text{O}_4(\text{O}_2\text{PPh}_2)_6]$ where all Mn...Mn separations are in the range 2.904–2.954 Å.⁹ The presence of hydrogen bonding in **3** between the μ_3 -OH[–] and an

(8) Dried solid analyzed as $3 \cdot \text{Et}_2\text{O} \cdot 1.7\text{CH}_2\text{Cl}_2$. Anal. Calcd (found): C, 50.4 (50.4); H, 4.2 (4.2). Crystal data for $3 \cdot 0.9\text{Et}_2\text{O} \cdot 1.1\text{CH}_2\text{Cl}_2$: monoclinic, $P2_1/c$, $a = 14.478(5)$ Å, $b = 14.910(5)$ Å, $c = 26.644(8)$ Å, $\beta = 101.00(2)^\circ$, $Z = 4$, $V = 5646$ Å³, $d_{\text{calc}} = 1.518$ g cm^{–3}, $T = -171$ °C; $R(F) = 7.84$ and $R_w(F) = 7.57\%$ using 4836 unique reflections with $F > 3\sigma(F)$.

Et₂O group (O...O = 2.951(16) Å) confirms the protonated nature of O(8). The X[–] groups in **1–3** lie on the three Mn^{III} Jahn–Teller elongation axes, and the resulting enhanced lability undoubtedly facilitates the site-specific substitution at this position. The process described in eq 1 is driven by the large excess (~300 equiv) of MeOH and the resulting shorter, stronger Mn^{III}–O_X bonds (table) even though the acidity of MeOH ($\text{p}K_a = 15.5$) is much less than MeCO₂H (4.8). The conversion in eq 2 is favored by the relative acidity of MeOH ($\text{p}K_a = 15.5$) versus H₂O ($\text{p}K_a = 14$) and such a large excess of H₂O is not necessary. We currently believe the substitutions occur via an intermediate whereby the μ_3 -X[–] (X[–] = MeCO₂[–] or MeO[–]) group becomes μ_2 -X[–] as the incoming group binds to one Mn^{III} site, followed by loss of XH as the new group is deprotonated and adopts a μ_3 mode.

Magnetic susceptibility data (2.00–300 K) on powdered samples of **2** and **3** were fit to the appropriate theoretical χ_m vs T expression for a C_{3v} symmetry Mn^{III}₃Mn^{IV} unit,^{3a,10} and the fitting parameters, in the format (J_{34} , J_{33} , g), were -31.8 cm^{–1}, $+9.6$ cm^{–1}, and 1.92 for **2** and -32.7 cm^{–1}, $+11.9$ cm^{–1}, and 2.02 for **3**. These values are very similar to those for **1** (-33.9 cm^{–1}, $+5.4$ cm^{–1}, and 1.94) and other $[\text{Mn}_4\text{O}_3\text{X}]$ (X[–] = Cl[–], Br[–], F[–]) complexes.^{3,10} Complexes **1–3** thus all have $S = 9/2$ ground states.

Complexes **1–3** display quasi-reversible one-electron reductions at 0.39, 0.16, and 0.16 V vs SCE, respectively, when examined by DPV and CV in CH₂Cl₂ and quasi-reversible oxidations at 1.55, 1.22, and 1.26V. These changes with X[–] are consistent with the relative basicities of the latter as gauged by the above $\text{p}K_a$ values and show that HO[–] and MeO[–] facilitate access to a higher oxidation state compared with MeCO₂[–]. The conversion of free H₂O into a bound OH[–] in **3** without change to the Mn₄O₃ core and via H⁺ transfer to a MeCO₂[–] or MeO[–] leaving group could parallel a similar transformation following (or accompanying) a S_n -to- S_{n+1} oxidation in the WOC, where according to recent theories both the electron and H⁺ transfers are to the Y_z tyrosine radical.^{11,12} The hydrogen-bonded Et₂O group may also be considered a model of how a second H₂O molecule could interact with the OH[–] to give a $[\text{H}_2\text{O} \cdots \text{HO}^-]$ pair poised for subsequent multiple deprotonations and oxidative coupling to form O₂;¹³ such a system would also be consistent with data showing both a slowly and rapidly exchanging substrate molecule at the native site.¹⁴ Current studies thus include isolation of **1** (or related species) at the 4Mn^{III} oxidation level to study H₂O binding and concomitant oxidation/deprotonation steps and deprotonation of **3** either alone or as a consequence of an oxidation to the 2Mn^{III},2Mn^{IV} level.

Acknowledgment. This work was funded by NIH Grants GM 39083 (G.C.) and HL 13652 (D.N.H.).

Supporting Information Available: Data collection and refinement details and listings of atomic coordinates and thermal parameters for complexes **2** and **3** and fitting of $\chi_m T$ vs T data for **2** and **3** (46 pages, print/PDF). See any current masthead page for ordering information and Web access instructions.

JA9730573

(9) Ruettinger, W. F.; Campana, C.; Dismukes, G. C. *J. Am. Chem. Soc.* **1997**, *119*, 6670.

(10) Hendrickson, D. N.; Christou, G.; Schmitt, E. A.; Libby, E.; Bashkin, J. S.; Wang, S.; Tsai, H.-L.; Vincent, J. B.; Boyd, P. D. W.; Huffman, J. C.; Foltling, K.; Li, Q.; Streib, W. E. *J. Am. Chem. Soc.* **1992**, *114*, 2455.

(11) (a) Tang, X.-S.; Randall, D. W.; Force, D. A.; Diner, B. A.; Britt, R. D. *J. Am. Chem. Soc.* **1996**, *118*, 7638. (b) Gilchrist, M. L.; Ball, J. A.; Randall, D. W.; Britt, R. D. *Proc. Natl. Acad. Sci.* **1995**, *92*, 9545.

(12) (a) Tommos, C.; Tang, X.-S.; Warnecke, K.; Hoganson, C. W.; Styring, S.; McCracken, J.; Diner, B. A.; Babcock, G. T. *J. Am. Chem. Soc.* **1995**, *117*, 10325. (b) Hoganson, C. W.; Lydakakis-Simantiris, X.; Tang, X.-S.; Tommos, C.; Warnecke, K.; Babcock, G. T.; Diner, B. A.; McCracken, J.; Styring, S. *Photosyn. Res.* **1995**, *46*, 177.

(13) We have, in fact, been able to crystallize **3** with the OH[–] hydrogen-bonded to two H₂O molecules instead of one Et₂O; however, the quality of the crystallographic data is currently very poor.

(14) Messinger, J.; Badger, M.; Wydrzynski, T. *Proc. Natl. Acad. Sci. U.S.A.* **1995**, *92*, 3209.